SECURITY INFORMATION

CONFIDENTIAL

Copy
RM L53J30

NACA RM L53J30

RESEARCH MEMORANDUM

PRELIMINARY INVESTIGATION OF THE TOTAL-PRESSURE-RECOVERY

CHARACTERISTICS OF A SYMMETRIC AND AN ASYMMETRIC NOSE

INLET OVER A WIDE RANGE OF ANGLE OF ATTACK

AT SUPERSONIC MACH NUMBERS

By Howard S. Carter and Charles F. Merlet

Langley Aeronautical Laboratory
Langley Field, Va.

CLASSIFICATION CH... UNCLASSIFIED

LIBRARY COPY

DEC 11 1953

LANGLEY AERONAUTICAL LABORATORY
LIBRARY, NACA
LANGLEY FIELD, VIRGINIA

To.

NACA Res abs
v RN-121

effective
Oct. 14, 1957

By authority of_____Date

tm 7 11-15-57

CLASSIFIED DOCUMENT

This material contains information affecting the National Defense of the United States within the meaning of the espionage laws, Title 18, U.S.C., Secs. 793 and 794, the transmission or revelation of which in any manner to an unauthorized person is prohibited by law.

NATIONAL ADVISORY COMMITTEE
FOR AERONAUTICS
WASHINGTON
December 9, 1953

CONFIDENTIAL

NATIONAL ADVISORY COMMITTEE FOR AERONAUTICS

RESEARCH MEMORANDUM

PRELIMINARY INVESTIGATION OF THE TOTAL-PRESSURE-RECOVERY

CHARACTERISTICS OF A SYMMETRIC AND AN ASYMMETRIC NOSE

INLET OVER A WIDE RANGE OF ANGLE OF ATTACK

AT SUPERSONIC MACH NUMBERS

By Howard S. Carter and Charles F. Merlet

SUMMARY

A preliminary investigation was made of the total-pressure-recovery characteristics over a wide range of angle of attack of an axially symmetric nose inlet at a Mach number of 1.42 and of an asymmetric nose inlet at Mach numbers of 1.42 and 1.84. The symmetric inlet had a maximum total-pressure recovery of 0.95 over the angle-of-attack range between $\pm 6^\circ$ for all mass-flow ratios tested. Static-pressure distributions and total-pressure profiles in the symmetric inlet duct indicated that at large angles of attack, severe separation occurred reducing the recovery as much as 12 percent at 20° angle of attack.

At a Mach number of 1.42, the total-pressure recovery of the asymmetric inlet was equal to or better than free-stream normal shock recovery for all angles of attack between 0° and 22°, reaching a maximum of 0.97, about 2 percent greater than normal shock recovery. At a Mach number of 1.84, however, the total-pressure recovery was as high as normal shock recovery only in the region of 10° angle of attack and was relatively insensitive to increasing angle of attack above 10°, while it was quite sensitive to decreasing angle of attack below 10°.

INTRODUCTION

Existing data (for example, ref. 1) have shown that the total-pressure recovery of a symmetric inlet is affected adversely by operation at angle of attack. In general, separation of the flow from the internal lower lip of the inlet at angle of attack results in lower total-pressure recovery after diffusion as well as reducing the maximum

flow rate achieved. The severity of the separation is in part dependent on the angle of attack and the amount of internal rounding of the lip.

In an attempt to obtain improved recovery over an angle-of-attack range, a preliminary investigation has been conducted on the total-pressure-recovery characteristics of an asymmetric inlet. The inlet plane was skewed at an angle of 45°. The inlet had sharp lips and a contraction ratio of 1. It was reasoned that, at positive angles of attack, the forward location of the upper lip (as a result of tilting the inlet plane) would produce a compression wave at supersonic speeds which would aid in turning the flow towards the diffuser axis as well as improve the pressure recovery by furnishing some supersonic compression.

Reference 2 presents data at 0° angle of attack for a convergent-divergent inlet with the inlet plane skewed 45°. Herein are presented the results from preliminary tests of a 45° skewed inlet at both a Mach number M of 1.42 and 1.84 over a wide range of angle of attack. For comparison, total-pressure recovery at angle of attack at M = 1.42 is also presented for a symmetric inlet having slightly rounded lips.

The Reynolds number for all tests at M = 1.42 was about 2.2×10^6 and for all tests at M = 1.84 was about 2.7×10^6, based on the inlet diameter normal to the axis of the inlet. All tests were made in the preflight jet of the Langley Pilotless Aircraft Research Station at Wallops Island, Va.

SYMBOLS

A	projected area on a plane perpendicular to the model center line, sq in.
α	angle of attack, deg
D	diameter, in.
γ	ratio of specific heats (1.40 for air)
H	local total pressure, lb/sq ft
$\overline{H}$	average total pressure, lb/sq ft
M	Mach number
$\dfrac{m}{m_0}$	ratio of mass flow through the duct to that flowing through a free-stream tube of the same area as the inlet area A_i

p   static pressure, lb/sq ft

x   horizontal distance along a diameter measured from the side
            of the duct at the rake station (see fig. 5), in.

y   vertical distance along a diameter measured from the upper-
            most point of the duct at the rake station (see figs. 3,
            4, and 5), in.

Subscripts:

e   model exit station (see figs. 3, 4, and 5)

i   model inlet station (see figs. 3, 4, and 5)

o   free stream, at free-jet exit

r   model rake station (see figs. 3, 4, and 5)

APPARATUS, INSTRUMENTATION, AND TESTS

A sketch and a photograph showing the arrangement of the testing
apparatus with the asymmetric inlet in place are presented as figures 1
and 2, respectively. A motor, cable, and pulley system were used to
rotate the inlet through the angle-of-attack range in the horizontal
plane. However, for convenience and clarity, it shall be assumed that
the angle of attack was varied vertically in the conventional manner.
Thus the long side of the asymmetric inlet shall be called the top, the
short side the bottom, and so forth.

A sectional view of the symmetric inlet showing instrumentation,
inlet support, and exit orifice plate is shown in figure 3. The axis
of rotation which passed through the inlet plane is indicated. The
inlet was made of brass, the inlet support of steel, and the exit ori-
fice plate of steel. The inlet lips were rounded inside and outside
in an attempt to reduce separation at large angles of attack. The
inlet discussed herein is identical with the corresponding portion of
the inlet tested in reference 3.

Static pressure orifices were installed in the symmetric inlet as
shown in figure 3. A seven-tube total-pressure rake and four individual
total-pressure tubes were installed at station 4 (section B-B) as shown,
The duct area at station 4 was 1.27 times the inlet minimum area. Three
orifice plates with ratios of exit to inlet area A_e/A_i of 0.94, 0.89,
and 0.85 were used to obtain data at different mass-flow ratios.

A sectional view of the asymmetric inlet as it was tested at M = 1.42, showing instrumentation, inlet support, and exit orifice plate is presented in figure 4. The axis of rotation is also indicated. The complete configuration was made of steel.

Two diametrically opposite static-pressure orifices were installed at section A-A (fig. 4). A five-tube total-pressure rake and two individual total-pressure tubes were installed at station 5.50 (section B-B) at the end of a constant area section. Three orifice plates with ratios of exit to inlet area A_e/A_i of 1.00, 0.95, and 0.90 were used with this configuration to obtain data at different mass-flow ratios.

A sectional view of the asymmetric inlet, as it was tested at M = 1.84, showing axis of rotation, instrumentation, inlet support, and exit nozzle block is presented in figure 5. The same inlet and inlet support were used in these tests at M = 1.84 as were used in the tests at M = 1.42. An aluminum liner was installed in the inlet support to make a conical diffuser. A seven-tube total-pressure rake and three individual total-pressure tubes were installed at the after end of the diffuser where the area ratio was 1.4 to 1 (fig. 5, section A-A). Three nozzle blocks with ratios of exit to inlet area A_e/A_i of 0.90, 0.85, and 0.80 were used with this configuration to obtain data at different mass-flow ratios.

All tests were made in the preflight jet of the Langley Pilotless Aircraft Research Station at Wallops Island, Va. (See ref. 4.) Two 8-inch-diameter nozzles with exit Mach numbers of 1.42 and 1.84 were used. The inlets were located with the axis of rotation of the inlet (see figs. 3, 4, and 5) approximately 1 inch downstream from the nozzle exit plane. During each test, the inlet was varied in angle of attack in steps of approximately 3°. The inlet was held at each angle of attack long enough to reach steady-state conditions. All pressures were measured with mechanical-optical pressure recorders, and time histories were recorded on film.

METHOD OF ANALYSIS

Mass-flow ratio and total-pressure recovery for each of the three configurations were computed by numerical integration of the Mach number

and total-pressure distributions obtained from the rake measurements. The two equations used were:

$$\frac{m}{m_o} = \frac{\int_{A_r} p_r M_r \left(1 + \frac{\gamma - 1}{2} M_r^2\right)^{1/2} dA}{p_o M_o \left(1 + \frac{\gamma - 1}{2} M_o^2\right)^{1/2} A_i}$$

$$\frac{\overline{H}_r}{H_o} = \frac{1}{A_r} \int_{A_r} \frac{H_r}{H_o} dA$$

Because of the limited instrumentation, the mass-flow ratios and pressure recoveries calculated for high angles of attack where severe separation occurred are not as accurate as the mass-flow ratios and recoveries for angles of attack with no separation. The angle of attack is believed to be accurate within 0.2^o. The probable accuracy of the other data is shown in the following tables for the two inlet configurations:

Probable accuracy for symmetric inlet:

	$\alpha = 0^o$	$\alpha = 20^o$	$\alpha = -20^o$
m/m_o . . .	± 0.02	± 0.05	± 0.05
$\overline{H}_r/H_o$ . . .	± 0.01	± 0.05	± 0.05
p/H_o . . .	± 0.01	± 0.01	± 0.01

Probable accuracy for asymmetric inlet:

	$\alpha = 0^o$	$\alpha = 20^o$	$\alpha = -20^o$
m/m_o . . .	± 0.02	± 0.03	± 0.05
$\overline{H}_r/H_o$ . . .	± 0.01	± 0.02	± 0.05
p/H_o . . .	± 0.01	± 0.01	± 0.01

▄▄▄▄▄

RESULTS AND DISCUSSION

Results are presented of tests of the symmetric inlet and the asymmetric inlet at a free-stream Mach number of 1.42 and comparisons are made. Data pertaining to the asymmetric inlet at a free-stream Mach number of 1.84 are presented to indicate the effect of a higher Mach number on the internal flow performance of the asymmetric inlet.

Although the angle of attack of the models tested was varied about a vertical axis, in order to be consistent with the usual concept of angle of attack varying about a horizontal axis, the data are discussed as if the long side of the asymmetric inlet is the top of the inlet. Hence, a positive angle of attack results when the long side of the inlet is pitched up.

Axially Symmetric Inlet, M = 1.42

Figure 6 presents the mass-flow ratio and total-pressure recovery as a function of angle of attack for the axially symmetric inlet at M = 1.42. For all three exit sizes tested, the mass-flow ratio and total-pressure recovery were symmetric with angle of attack. Since fixed exit areas were used, the mass flow decreased as the losses increased. At $\alpha = 0^\circ$, for $A_e/A_i = 0.94$, the mass-flow ratio was 0.96, the maximum allowed by the inlet contraction ratio at the test Mach number, whereas for $A_e/A_i = 0.89$ and 0.85, the mass-flow ratios were 0.90 and 0.85, respectively (fig. 6(a)).

At $\alpha = 0^\circ$, the total-pressure recovery (fig. 6(b)) was about 0.95, a value slightly less than free-stream normal-shock recovery, for all flow rates tested, indicating that the diffuser losses were small and essentially independent of flow rate in this range of mass-flow ratio. The diffuser losses would be expected to be small and essentially independent of flow rate, considering the short distance to the rake (about 1.4 inlet diameters), the small area ratio of the diffuser (1.3 to 1), and the small range of mass-flow ratios tested. The data presented in reference 3, obtained from flight tests at $\alpha = 0^\circ$, indicated that the total-pressure recovery measured at the end of a diffuser with an area ratio of 2.3 to 1 and a length of approximately 10 inlet diameters was 0.94 for a mass-flow ratio of 0.9 at this Mach number. If the difference in diffusers is considered, the agreement is good.

Maximum recovery was maintained for an angle-of-attack range of $\pm 6^\circ$, $\pm 8^\circ$, and $\pm 10^\circ$ for $A_e/A_i = 0.94$, 0.89, and 0.85, respectively. Above these angles, internal separation caused the recovery to drop as angle of attack increased. Apparently the increased curvature of the entering

streamlines and the reduced pressure gradient along the diffuser at
reduced flow rates tended to delay separation until higher angles of
attack were reached. Thus the recovery was somewhat greater at reduced
mass flows at the higher angles of attack.

Figure 7 presents some total-pressure distributions at the rake
station of the symmetric inlet. At $\alpha = 0^{\circ}$ (fig. 7(a)), the profile
was uniform for all flow rates. For $A_e/A_i = 0.94$, above $\alpha = 6^{\circ}$, the
profile became asymmetric and a low pressure-recovery region appeared
along the bottom side of the diffuser indicating separation. At
$\alpha = 20.4^{\circ}$ (fig. 7(b)) the separation was quite severe and the low
pressure region extended over approximately half the diffuser. Reducing
the flow rate delayed the appearance of separation and reduced its
severity at the higher angles of attack, as indicated in figure 7(b)
for $A_e/A_i = 0.85$.

Pressure distributions along the top and bottom wall of the dif-
fuser are presented as a ratio of p/H_0 in figure 8. At $\alpha = 0^{\circ}$
(fig. 8(a)) the static pressure was essentially equal along the top
and bottom walls at all stations for all flow rates. For $A_e/A_i = 0.94$,
at $\alpha = 6.5^{\circ}$, the pressure along the lower wall had dropped considerably
in the region of the inlet minimum area station, as required to turn
the air. The pressure gradient along the lower wall became more adverse,
and a local region of supersonic velocities was indicated. At $\alpha = 14.5^{\circ}$
and 20.4° (figs. 8(c) and 8(d)) the region has disappeared indicating
that the flow has separated from the lower lip at these higher angles.
For the smaller exit size, the static-pressure distribution showed less
adverse gradient at any given angle, and the flow remained attached to
higher angles of attack than for the larger exit.

Asymmetric Inlet, $M = 1.42$

The mass-flow ratio and total-pressure recovery of the asymmetric
inlet are presented in figure 9 as functions of angle of attack for
$M = 1.42$. The mass-flow ratio as presented is based on constant inlet
area equal to the projected inlet area at $\alpha = 0^{\circ}$. The three exits
used reached the point of maximum mass flow at approximately $\alpha = 3^{\circ}$.
At $\alpha < 3^{\circ}$, the mass-flow ratio dropped quite rapidly, while at $\alpha > 3^{\circ}$,
there was only a slight decrease in mass flow.

Maximum total-pressure recovery of 0.97 occurred at about $\alpha = 5^{\circ}$,
a value about 2 percent greater than normal shock recovery. For nega-
tive angles of attack, the recovery dropped quite rapidly. At these
angles, expansion around the long lip increased the shock losses, and
separation from the long lip increased the losses within the diffuser.
At $\alpha > 5^{\circ}$, however, the recovery decreased much more gradually. The

recovery was 0.95 or higher from $\alpha = 0^\circ$ to $\alpha = 22^\circ$, and at $\alpha = 35^\circ$, it was still about 0.92. Throughout the positive angle-of-attack range, the total-pressure-recovery was essentially independent of mass-flow ratio for the range of flow rates tested.

Some typical total-pressure recovery distributions for the asymmetric inlet are presented in figure 10. As the angle of attack increased, the distribution became more uniform, as shown by comparing figure 10(a) for $\alpha = 0^\circ$ with figure 10(b) for $\alpha = 10.9^\circ$. The profile remained nearly uniform up to $\alpha \approx 20^\circ$. At $\alpha = 22.8^\circ$ (fig. 10(c)) the profile shows the beginning of a low pressure region, probably caused by separation from the short lip. At large negative angles of attack, however (fig. 10(d)), the separation was quite severe, and the low pressure region extended almost completely across the duct. As in the case of the symmetric inlet, reducing the flow rate tended to delay separation at positive angles of attack, as shown in figure 10(c) for $A_e/A_i = 1.00$ and 0.90. At negative angles of attack, however, the flow seemed as badly separated for all flow rates tested.

In contrast to the symmetric inlet, the mass-flow ratio and total-pressure recovery of the asymmetric inlet varied at small angles of attack. The maximum total-pressure recovery of the two inlets is compared in figure 11. At all positive angles of attack, the asymmetric inlet had higher pressure recovery. At $\alpha = 5^\circ$, the asymmetric inlet had about 2.3 percent more recovery and at $\alpha = 20^\circ$, it was about 8 percent better. Furthermore, the recovery of the asymmetric inlet at $\alpha = 24^\circ$ was as good as the maximum pressure recovery attained with the symmetric inlet. At negative angles, however, the asymmetric inlet had the lower recovery, being lower by 4 percent at $\alpha = -5^\circ$ and about 28 percent at $\alpha = -20^\circ$.

Asymmetric Inlet, M = 1.84

Because of the favorable total-pressure-recovery characteristics of the asymmetric inlet at positive angles of attack at $M = 1.42$, the tests were extended to include $M = 1.84$. For these tests, the rake station was moved back to the end of a 1.4- to -1 conical diffuser which had been added.

Mass-flow ratio and total-pressure recovery at $M = 1.84$ are presented in figure 12 as a function of angle of attack for the three exit sizes tested. Here again, as at $M = 1.42$, the mass-flow ratio was based on a constant inlet area, the projected inlet area at $\alpha = 0^\circ$. However, since the actual projected frontal area increases as angle of attack increases, the inlet attained mass-flow ratios greater than one. For all three exits, the maximum flow rate occurred at $\alpha = 10^\circ$.

The change in mass flow with change in angle of attack was similar to that observed at $M = 1.42$, dropping slightly for $\alpha > 10^{\circ}$, and decreasing rapidly for $\alpha < 10^{\circ}$.

The total-pressure recovery (fig. 12(b)) was again essentially independent of mass flow for the range of flow rates tested, and varied in a manner similar to the variation observed at $M = 1.42$. The maximum recovery of 0.80 occurred at $\alpha = 10^{\circ}$, decreasing slowly as angle of attack increased until at $\alpha = 30^{\circ}$, the recovery was 0.77. Thus, the recovery only dropped about 4 percent for a 20° change in angle of attack. As angle of attack decreased below 10°, however, the recovery dropped rapidly until at $\alpha = -10^{\circ}$ it was 0.52, a decrease of nearly 40 percent. As was true at $M = 1.42$, the low recovery at negative angles resulted from the increased shock losses due to the expansion around the long lip and losses caused by severe separation occurring at the inlet lip, whereas the flow remained more uniform at the higher positive angles of attack. It should also be noted that the maximum recovery of 0.80 is approximately equal to the free-stream normal shock recovery, and that the recovery did not exceed this value as it did at $M = 1.42$.

Some typical total-pressure-recovery distributions at $M = 1.84$ are presented in figure 13 for several angles of attack and for $A_e/A_i = 0.80$. The curves at the left of the figure present measurements made along the vertical diameter, whereas the curves at the right are from measurements along a horizontal radius. At $\alpha = -8.0^{\circ}$, separated flow occurred over a large portion on the duct. As angle of attack increased, the separated region became smaller and the losses were less severe until at $\alpha = 18.5^{\circ}$ the profile was nearly uniform. It is interesting to note that, between $\alpha = 7.4^{\circ}$ and 18.5°, a small region of the inlet had recovery greater than normal shock recovery near the upper wall of the diffuser, as did a local region near the lower wall at negative angles of attack. Thus, it appears possible that modification to the inlet design might produce an inlet having greater than normal shock recovery at this Mach number, and the need for further research is indicated.

CONCLUSIONS

An investigation of the total-pressure-recovery characteristics of an axially symmetric nose inlet at a Mach number of 1.42 and an asymmetric nose inlet at Mach numbers of 1.42 and 1.84 indicated the following conclusions:

1. At a mass-flow ratio of 0.96, the symmetric inlet had a total-pressure recovery of about 0.95, a value slightly less than normal shock recovery, for all angles of attack between -6° and 6°. Reducing the mass-flow ratio from 0.96 to 0.85 extended the range of maximum recovery up to 10° in either direction.

2. Large losses at higher angles of attack resulting from severe separation at the inlet lips reduced the recovery of the symmetric inlet as much as 12 percent at 20° angle of attack.

3. At a Mach number of 1.42, the asymmetric inlet had a total-pressure recovery equal to or better than free-stream normal shock recovery between 0° and 22° angles of attack for all flow rates tested. The maximum recovery was 0.97 at an angle of attack of 5°, a value about 2 percent higher than normal shock recovery.

4. At negative angles of attack, the recovery of the asymmetric inlet decreased rapidly, due to increased shock losses resulting from expansion around the long lip and to separation from the long lip of the inlet.

5. At Mach number of 1.84, the maximum total-pressure recovery of the asymmetric inlet occurred at an angle of attack of 10° and had a value of 0.80, about normal shock recovery.

6. At M = 1.84, the total-pressure recovery of the asymmetric inlet was also relatively insensitive to increasing angle of attack above 10°, and was quite sensitive to decreasing angles of attack below 10°.

Langley Aeronautical Laboratory,
      National Advisory Committee for Aeronautics,
            Langley Field, Va., October 15, 1953.

REFERENCES

1. Pendley, Robert E., Milillo, Joseph R., and Fleming, Frank F.: An Investigation of Three NACA 1-Series Nose Inlets at Subsonic and Transonic Speeds. NACA RM L52J23, 1953.

2. Dennard, John S., and Nelson, William J.: Preliminary Investigation of the Effect of Inlet Asymmetry on the Performance of Converging-Diverging Diffusers at Transonic Speeds. NACA RM L52J20, 1952.

3. Sears, Richard I., and Merlet, C. F.: Flight Determination of Drag and Pressure Recovery of a Nose Inlet of Parabolic Profile at Mach Numbers From 0.8 to 1.7. NACA RM L51E02, 1951.

4. Faget, Maxime A., Watson, Raymond S., and Bartlett, Walter A., Jr.: Free-Jet Tests of a 6.5-Inch-Diameter Ram-Jet Engine at Mach Numbers of 1.81 and 2.00. NACA RM L50L06, 1951.

Nozzle —⁊   — Asymmetric inlet

Cable —⁊

Fairing   Motor

Position recorder   H-beam
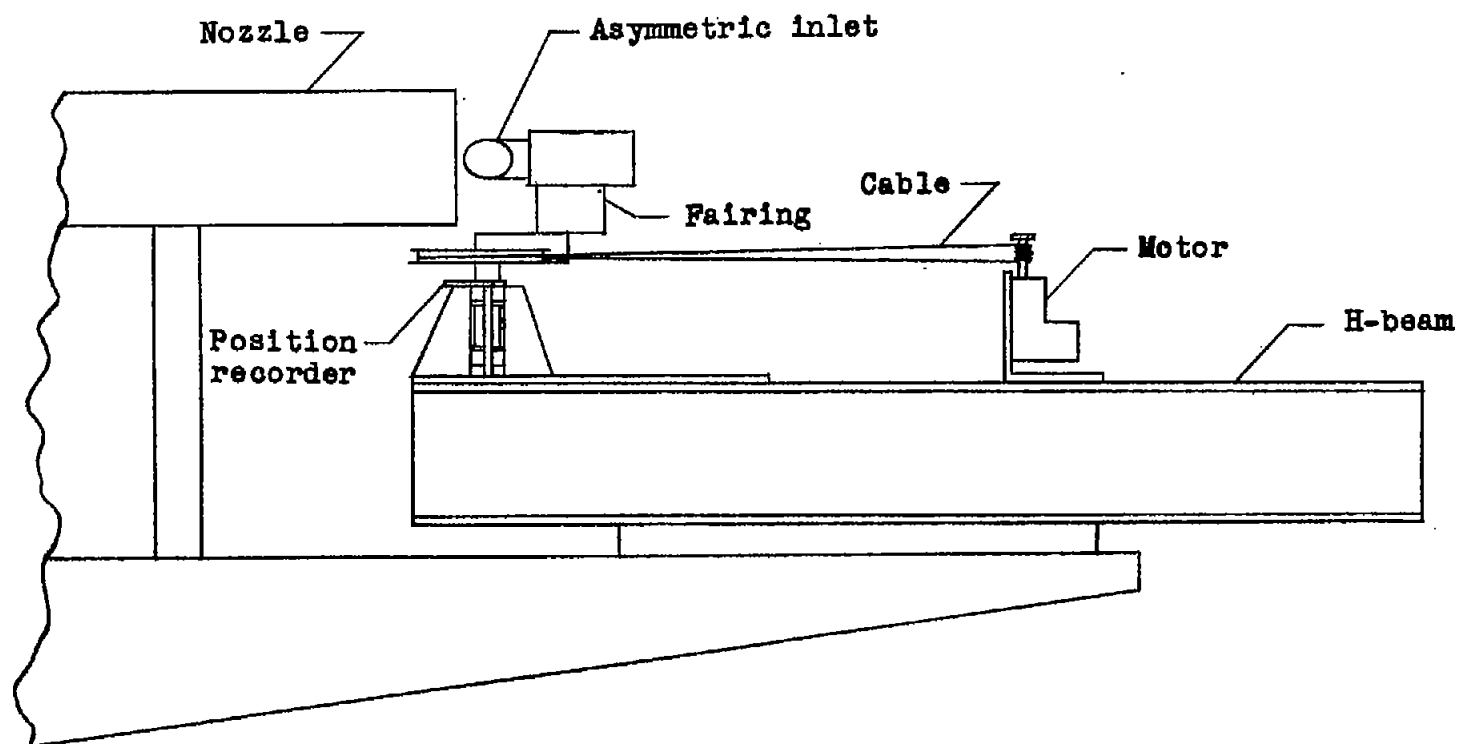
Figure 1.- Arrangement of the test apparatus showing the asymmetric inlet.
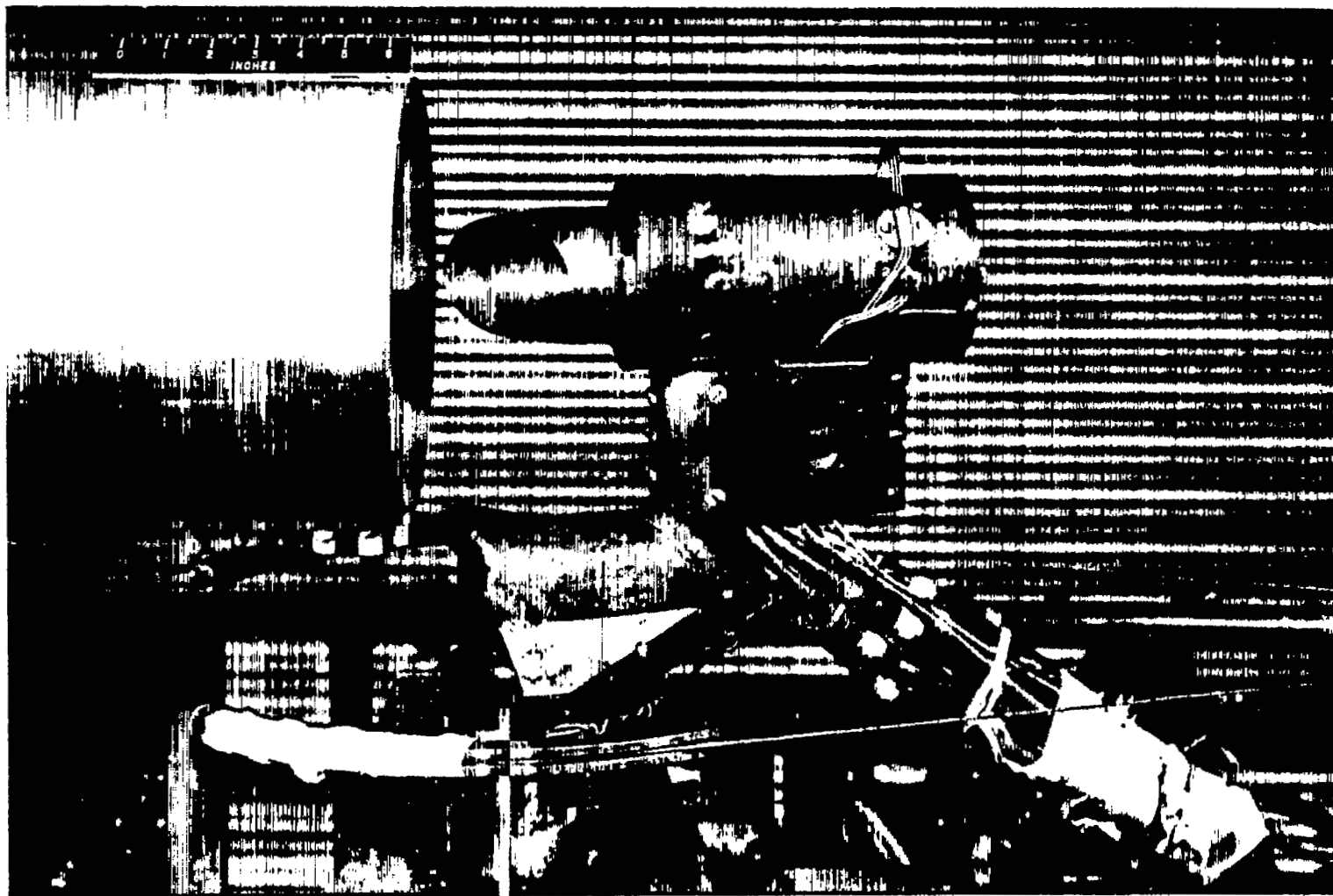
L-77726

Figure 2.- Test apparatus showing the asymmetric inlet.
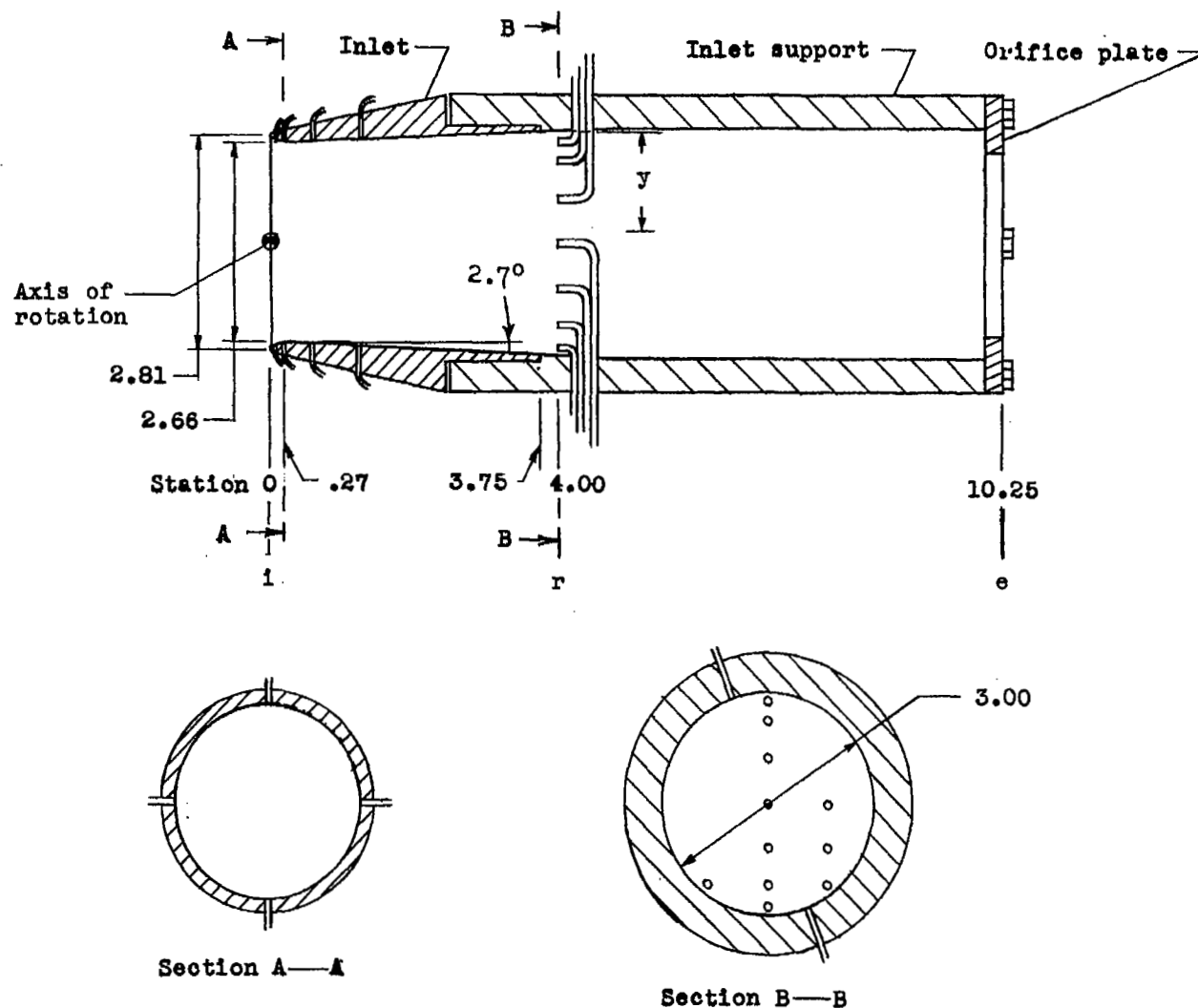
Figure 3.- Sectional view of the symmetric inlet showing instrumentation, inlet support, and exit orifice plate. All dimensions are in inches.

Figure 4.- Sectional view of the asymmetric inlet as it was tested at
.M = 1.42, showing instrumentation, inlet support, and exit orifice
plate. All dimensions are in inches.

Figure 5.- Sectional view of the asymmetric inlet as it was tested at
M = 1.84, showing instrumentation, inlet support, and exit orifice
plate. All dimensions are in inches.
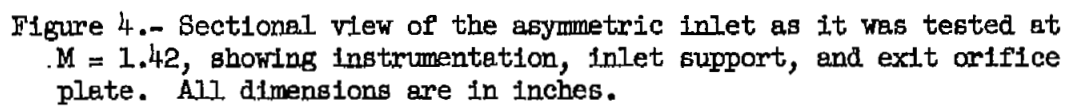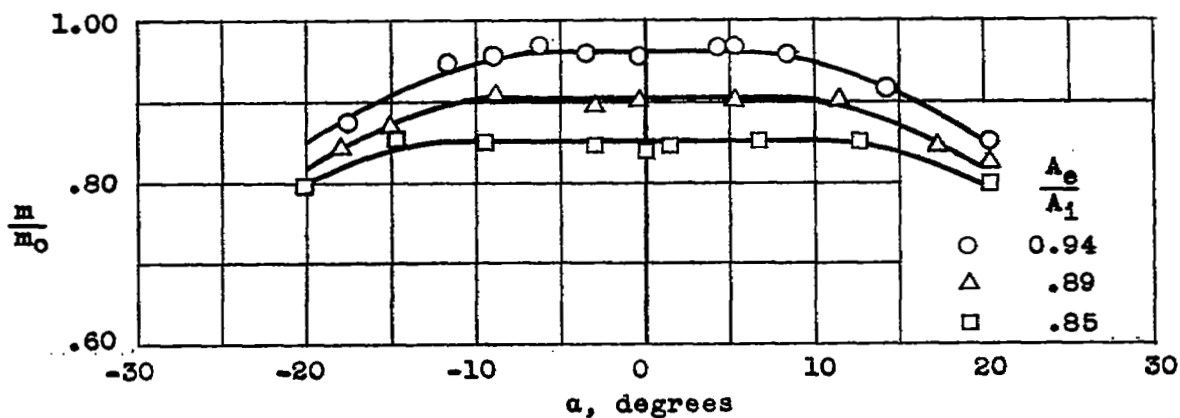
(a) Mass-flow ratio.
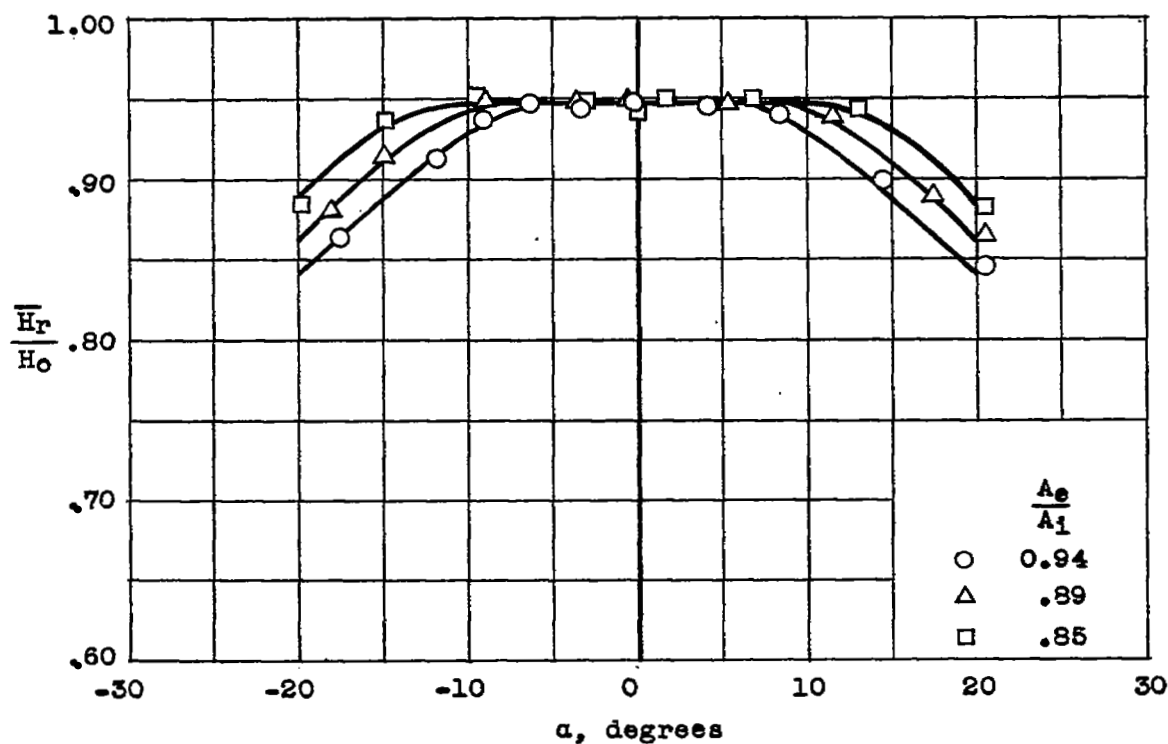
(b) Total-pressure recovery.

Figure 6.- Mass-flow ratio and total-pressure recovery of the symmetric
inlet as functions of angle of attack for three ratios of exit to
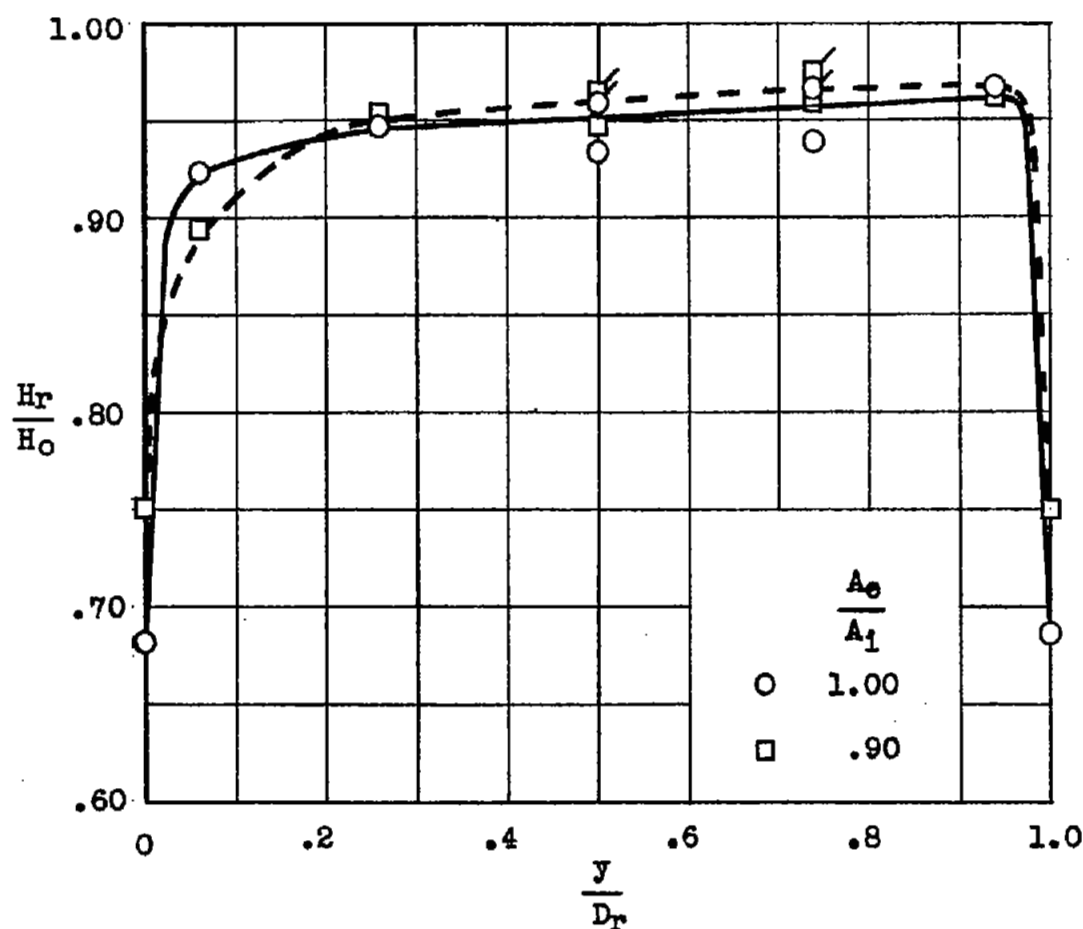inlet area at M = 1.42.
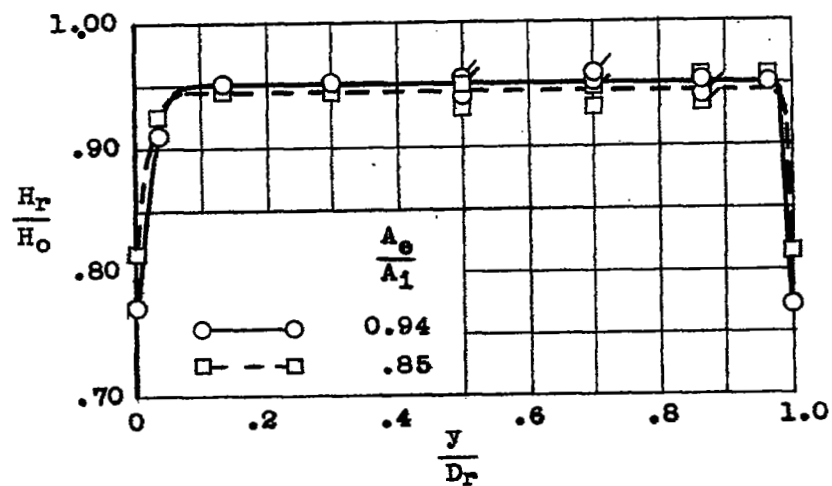
(a) $\alpha = 0^\circ$.
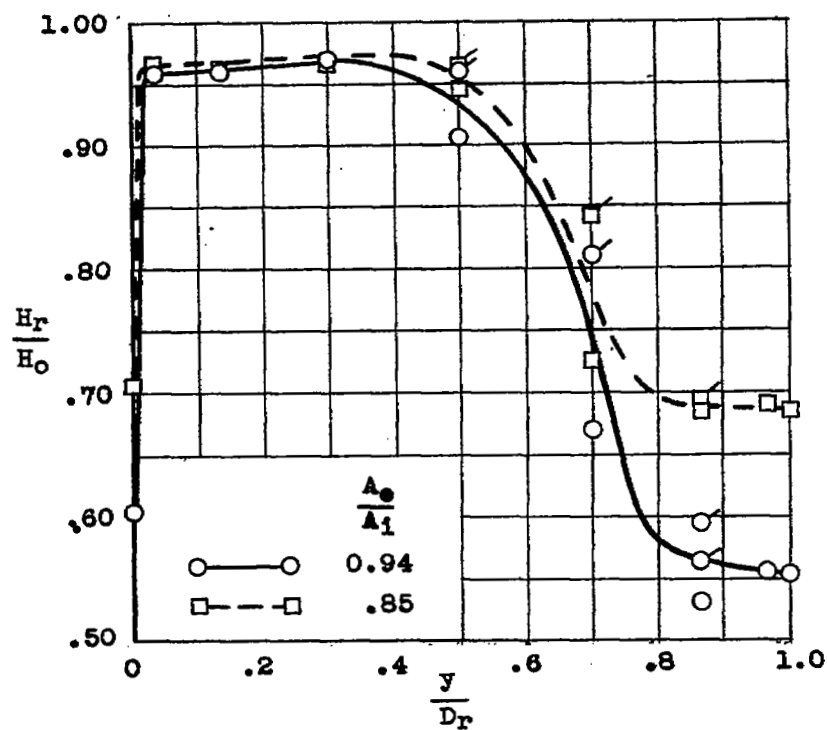
(b) $\alpha = 20.4^\circ$.

Figure 7.- Total-pressure distributions at the rake station of the symmetric
inlet for two angles of attack and two ratios of exit to inlet area at
M = 1.42. Flagged symbols represent measurements made out of plane of
rake.
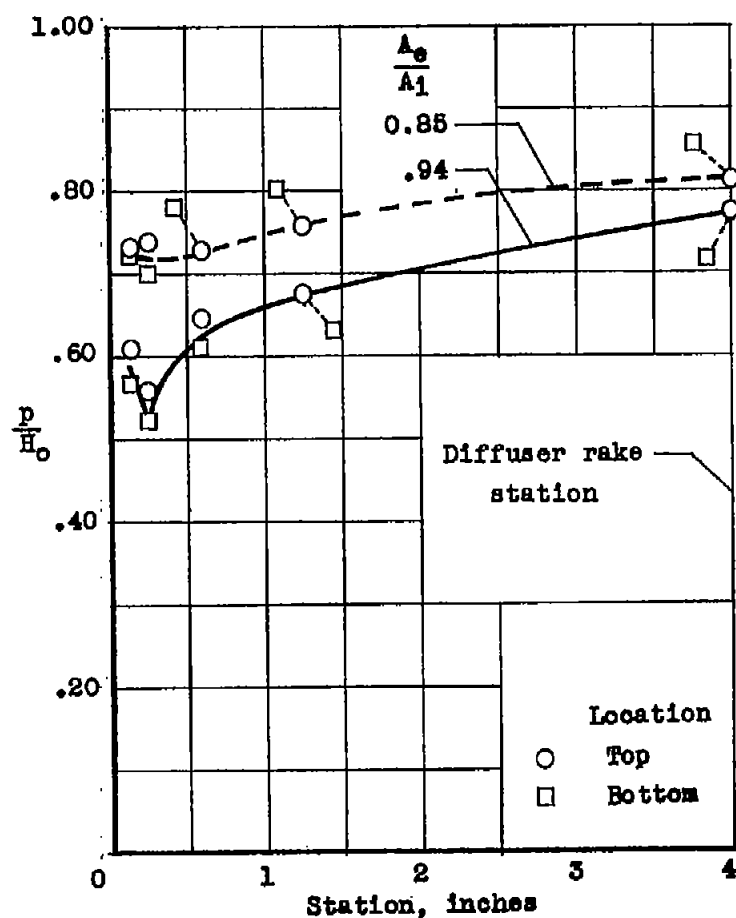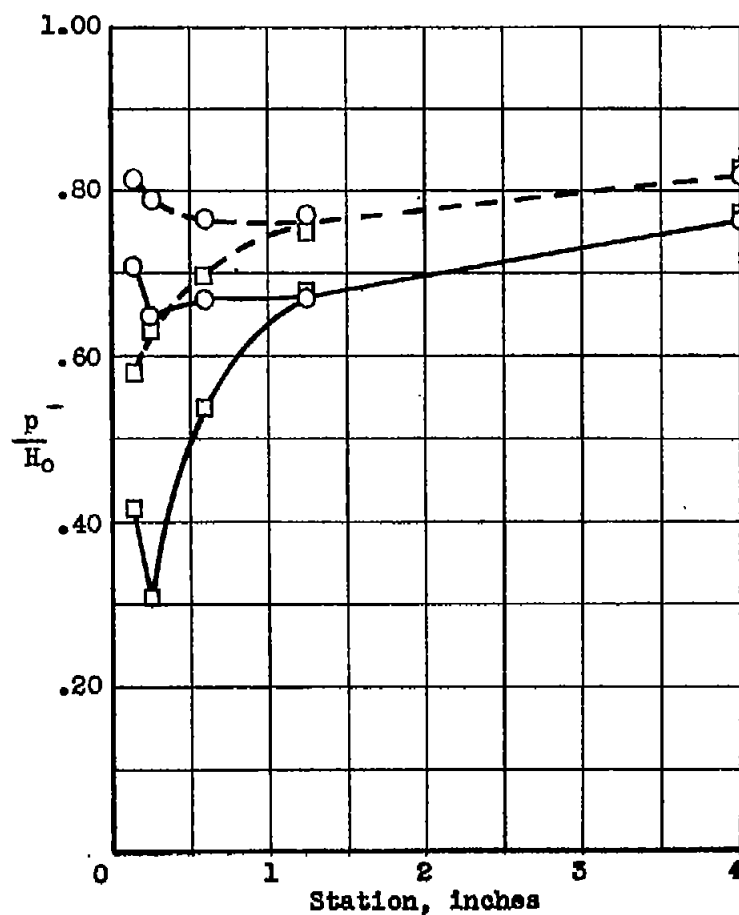
(a) α = 0°.　　　　　　　　　　(b) α = 6.5°.

Figure 8.- Static-pressure distributions along the inside top and bottom
of the symmetric inlet for four angles of attack and two ratios of
exit to inlet area at M = 1.42.
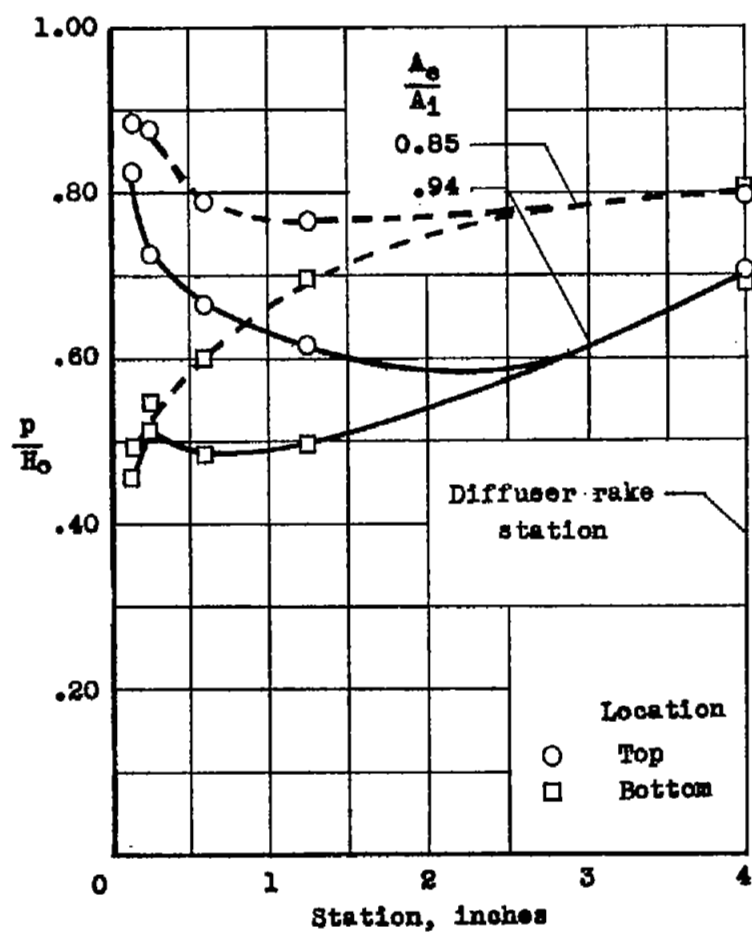
(c) $\alpha = 14.5^{\circ}$.
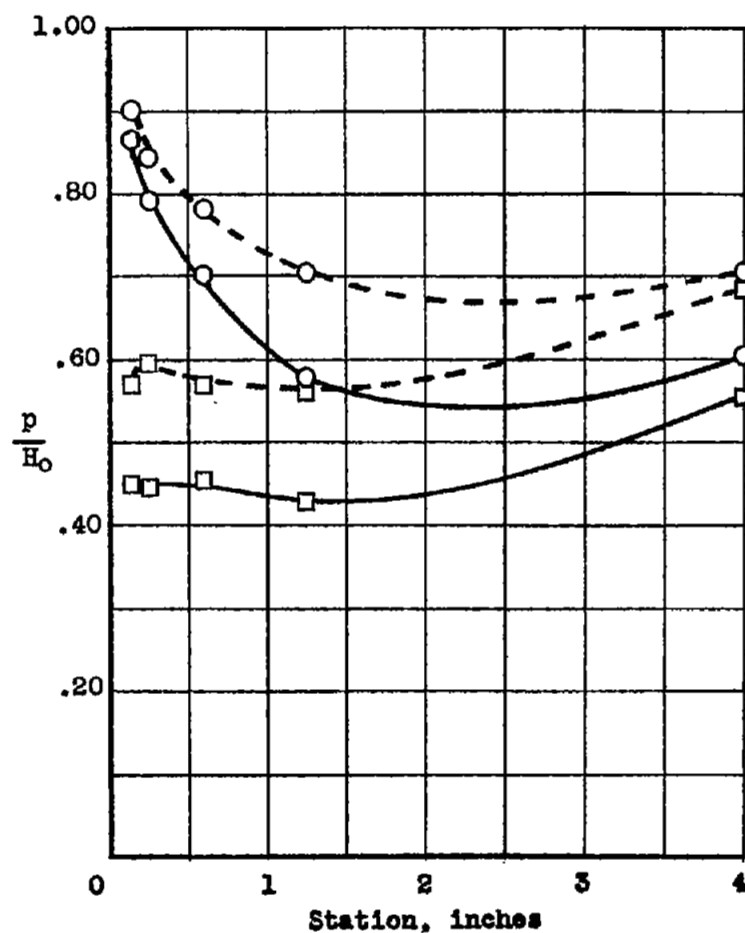
(d) $\alpha = 20.4^{\circ}$.

Figure 8.- Concluded.
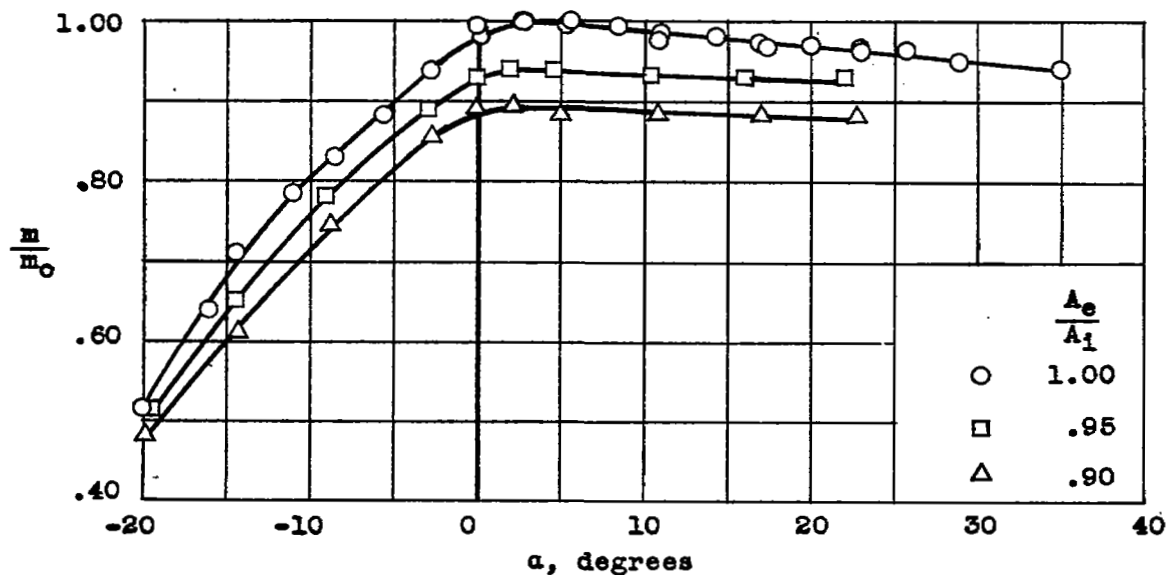
(a) Mass-flow ratio.
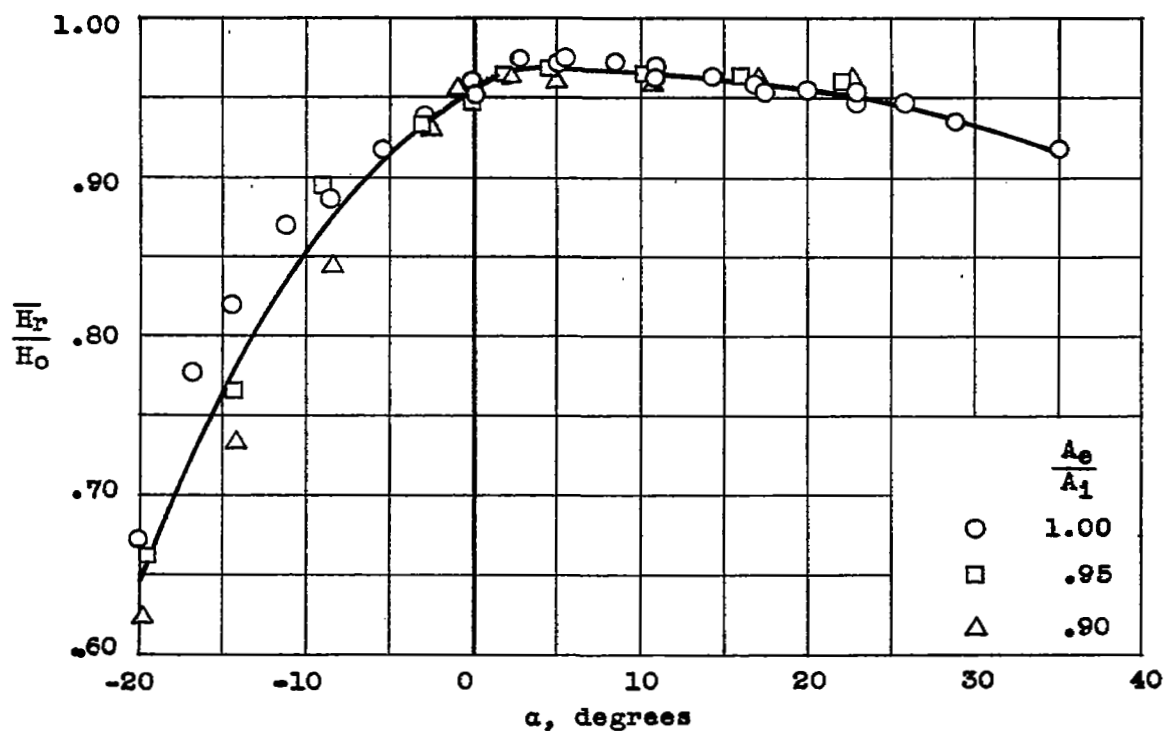
(b) Total-pressure recovery.

Figure 9.- Mass-flow ratio and total-pressure recovery of the asymmetric
inlet as functions of angle of attack at M = 1.42.

(a) α = 0°.

Figure 10.- Total-pressure distributions at the rake station of the asymmetric
inlet for four angles of attack as tested at M = 1.42. Flagged symbols
represent measurements made out of plane of rake.
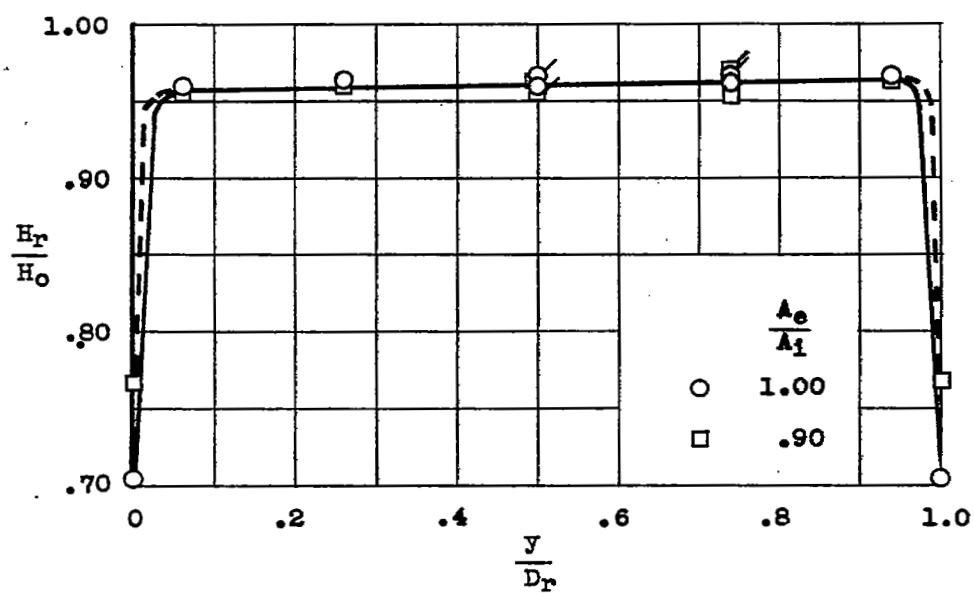
(b) $\alpha = 10.9°$.
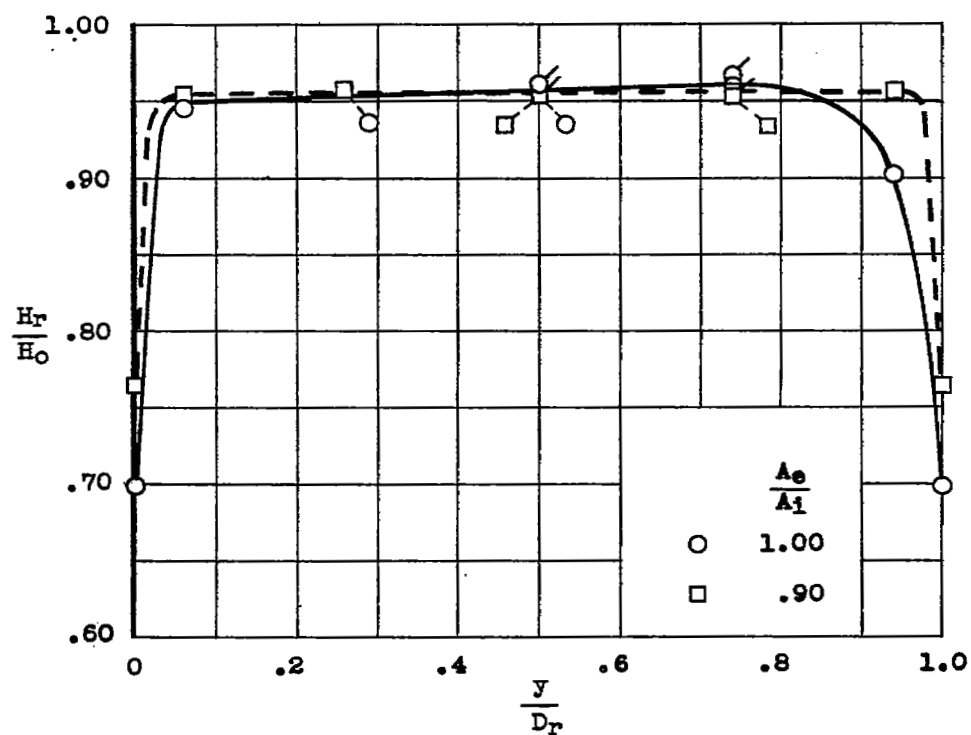
(c) $\alpha = 22.8°$.
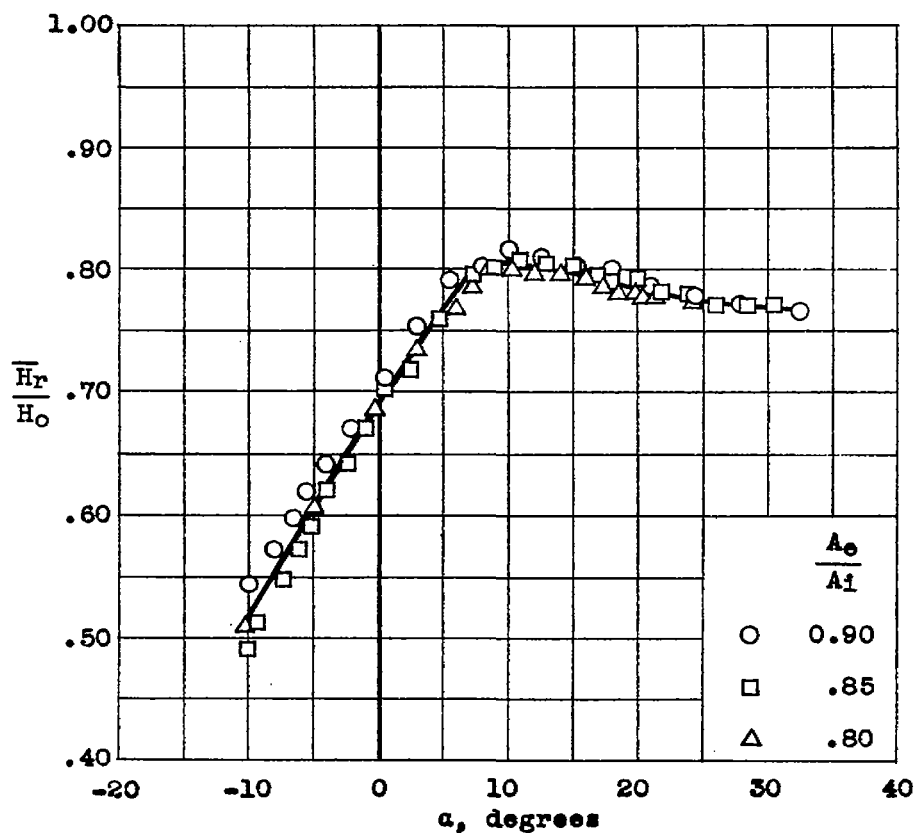
Figure 10.- Continued.

24
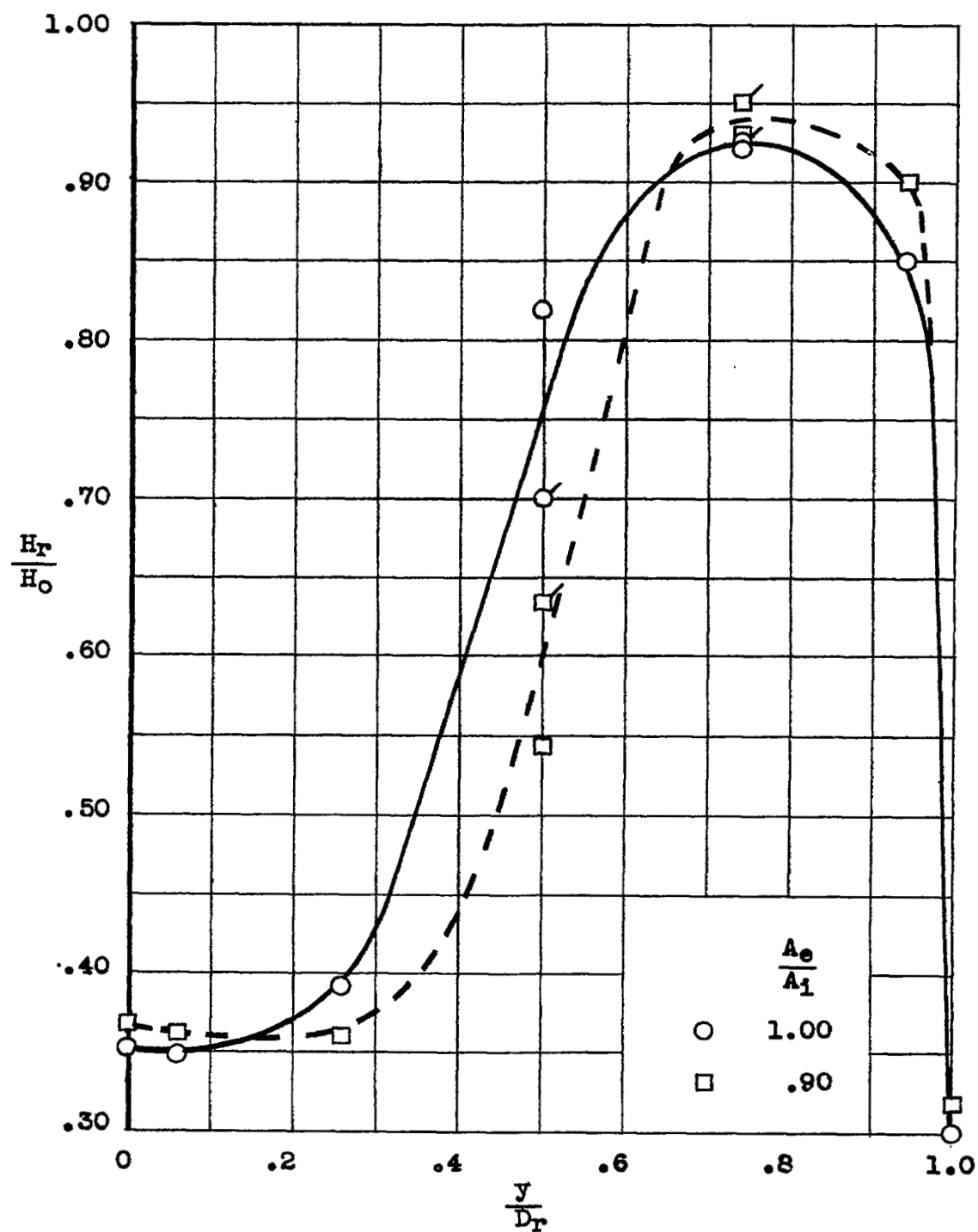
(d) $\alpha = -19.8°$.

Figure 10.- Concluded.
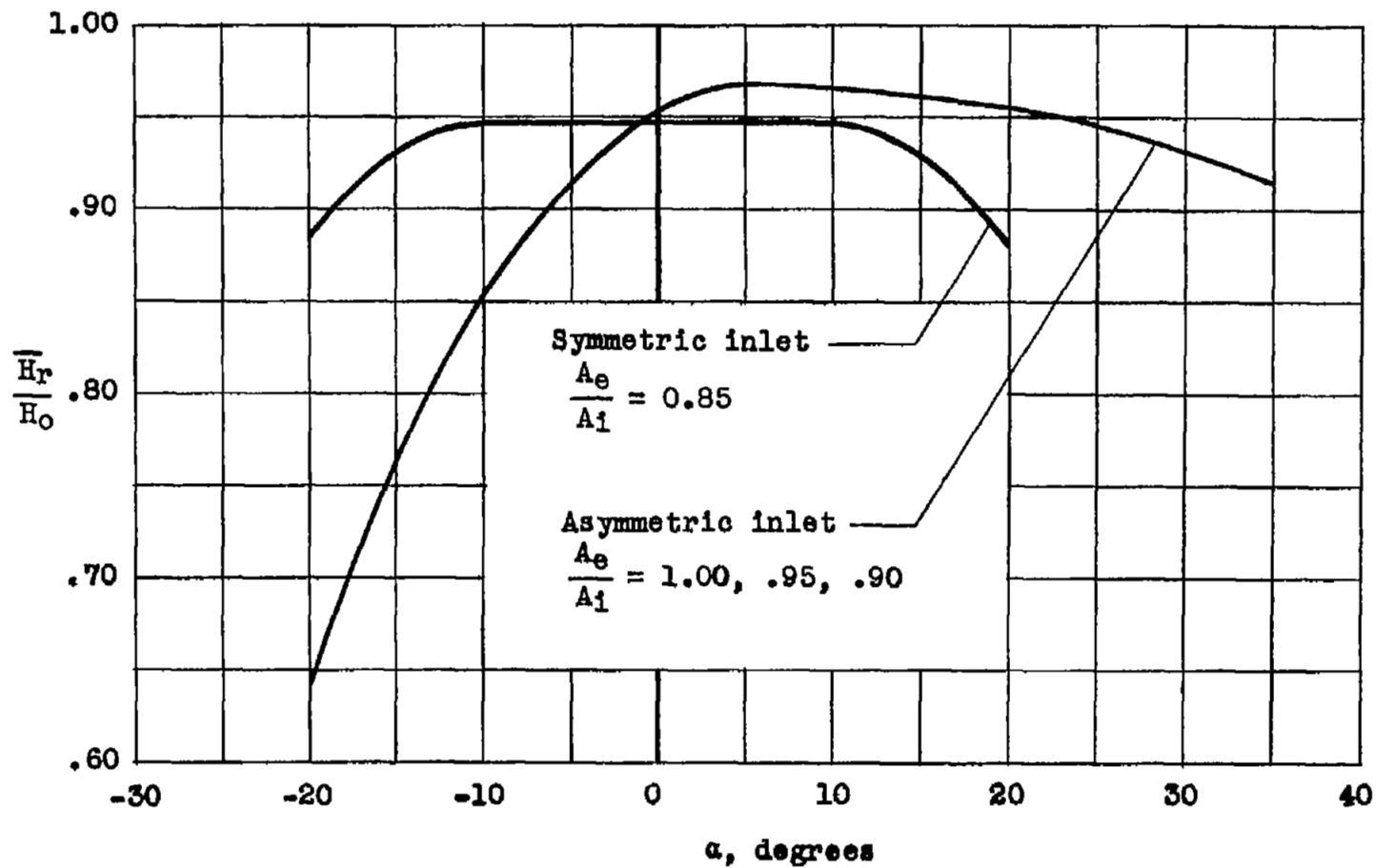
Figure 11.- Comparison of maximum pressure recovery of symmetric and asymmetric inlets as tested at M = 1.42.
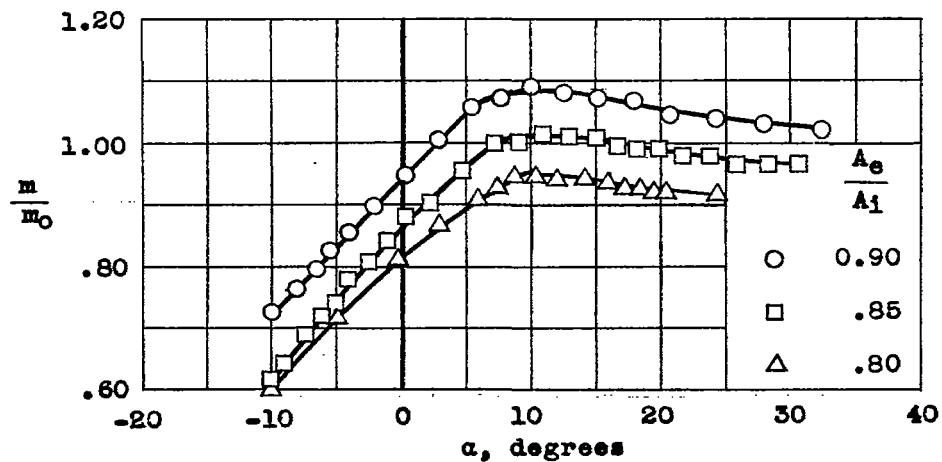
(a) Mass-flow ratio.

(b) Total-pressure recovery.

Figure 12.- Mass-flow ratio and total-pressure recovery of the asymmetric
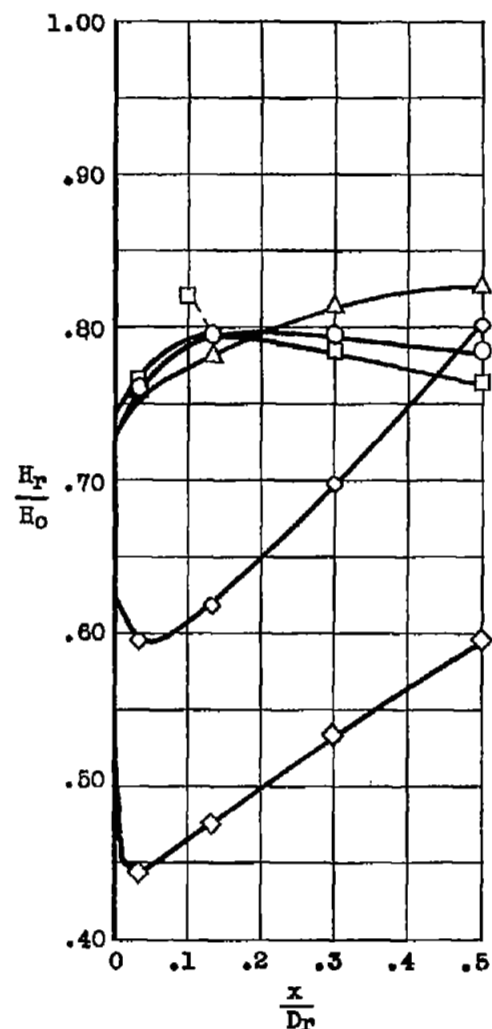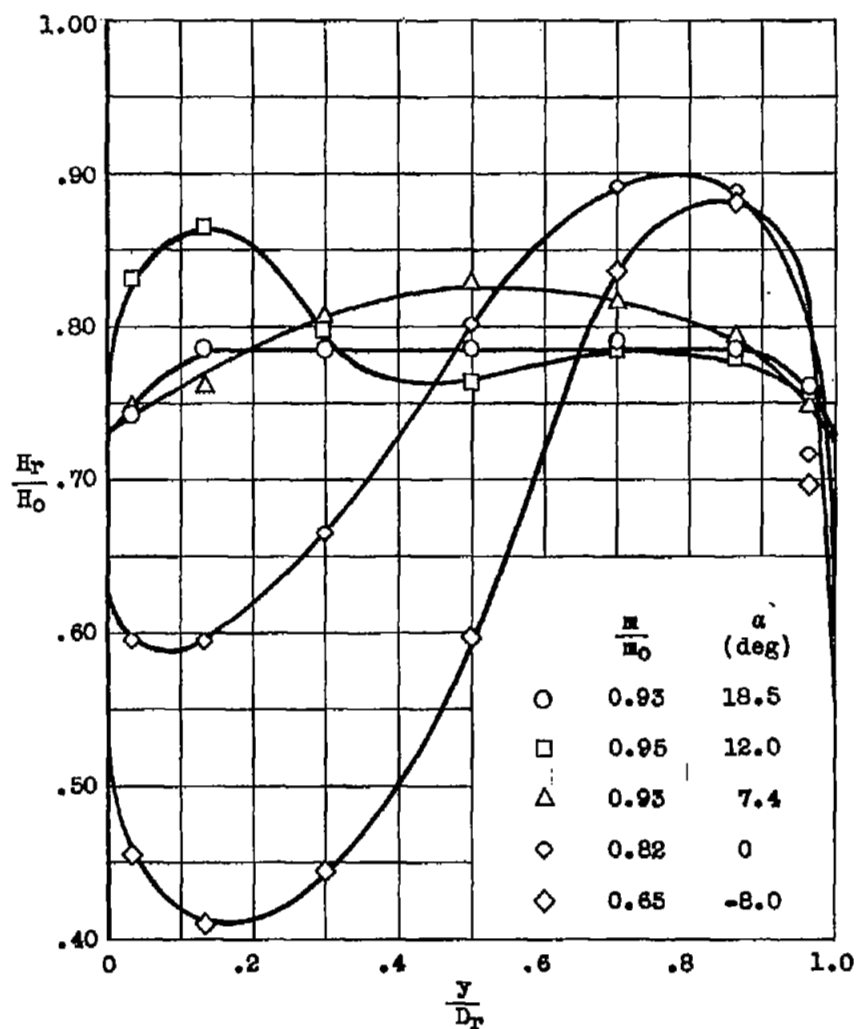inlet as functions of angle of attack at M = 1.84.

Figure 13.- Total-pressure distributions at the rake station of the asymmetric inlet for several angles of attack as tested at M = 1.84. $A_e/A_1 = 0.80$.